05

The influence of mechanical tensile deformation on the magnetoresistance of magnetic straintronics nanostructures

© D.A. Zhukov[1], O.P. Polyakov[2], P.A. Polyakov[2], V.V. Amelichev[1], S.I. Kasatkin[3], D.V. Kostyuk[1]

[1] Scientific-Manufacturing Complex „Technological Centre“, Zelenograd, Moscow, Russia
[2] Moscow State University, Moscow, Russia
[3] Trapeznikov Institute of Control Sciences, Russian Academy of Sciences, Moscow, Russia
E-mail: D.Zhukov@tcen.ru

Received April 18, 2025
Revised June 18, 2025
Accepted July 10, 2025

The results of experimental and theoretical studies of magnetic straintronics nanostructure Ta (5 nm)/FeNiCo (20 nm)/CoFe (10 nm)/Ta (5 nm) are presented. The magnetoresistance dependence on external magnetic field strength under the mechanical tensile deformation is determined. A theoretical model explaining the features of this experimental dependence is proposed. In particular, the experimentally established asymmetry of magnetoresistance variations under the compressive and tensile deformations is explained.

Keywords: magnetic straintronics, magnetoresistive effect, theory of micromagnetism, magnetoresistive nanostructure.

DOI: 10.61011/TPL.2025.10.62114.20349

One of important trends in modern nanoelectronics and spintronics is magnetic straintronics [1–3]. A typical magnetic straintronics nanostructure consists of magnetic nanolayers, one of which exhibits an enhanced inverse magnetostrictive effect. This allows controlling the state of its magnetic ordering and, hence, magnetoresistance [4] or giant magnetoresistance [5], by creating in this nanostructure a compressive or tensile deformation. The use of anisotropic magnetoresistive (AMR), spin-valve, and spin-tunnel magnetoresistive nanostructures in combination with magnetostrictive films enables creation of a new type of mechanical transducers possessing improved characteristics and expanded functionality [6,7].

In this work, we have investigated magnetoresistance of a magnetic straintronics nanostructure $3.8 \times 19.8 \times 0.46$ mm in size, which was formed on a silicon substrate and had the Ta (5 nm)/FeNiCo (20 nm)/$Co_{50}Fe_{50}$ (10 nm)/Ta (5 nm) structure consisting of the magnetoresistive (FeNiCo) and magnetostrictive (CoFe) layers. Experimental curves of the nanostructure magnetoresistance dependence on the external magnetic field directed at the angle of 45° to the easy-magnetization axis (EMA) in the presence of compressive and tensile deformation were obtained in [8]. A distinctive feature of these curves is strong asymmetry of the compressive and tensile deformation effects. The maximum magnetoresistance variation under the tensile deformation proved to be several times weaker than that under compressive deformation.

The paper presents a theoretical model for magnetization reversal of a magnetic straintronics nanostructure in the presence of tensile deformation. The proposed theory is well-consistent with the experimental nanostructure magnetoresistance dependence on the external magnetic field. In addition, the theory developed explains the above-mentioned asymmetry of the magnetoresistance variation under the compressive and tensile deformations.

Consider the proposed theoretical model. Let $\mathbf{M}_1$ and $\mathbf{M}_2$ be magnetization vectors of the considered nanostructure layers: magnetostrictive CoFe layer h_1 thick and magnetoresistive FeNiCo layer h_2 thick. Those vectors lie in the layer planes and are oriented in the same direction due to strong exchange interaction. Assume coordinate axis X to be directed along the long side of the nanostructure under consideration. Then the volumetric magnetic energy density of the first (magnetostrictive) layer will be defined as [4]

$$w_1 = K_1 \sin^2(\varphi - \beta) - \frac{3}{2}\sigma\lambda_1 \sin^2\varphi - H_x M_1 \cos\varphi, \quad (1)$$

where K_1 is the uniaxial anisotropy constant in this layer, φ is the angle between vector $\mathbf{M}_1$ and axis X, $\beta = \pi/4$ is the angle between EMA and axis X, σ is the applied stress, λ_1 is the magnetostrictive constant, H_x is the projection of the external magnetic field vector onto axis X. In the case considered, external magnetic field vector $\mathbf{H}$ is directed either along or against axis X.

The magnetic energy density of the second (magnetoresistive) layer is defined as

$$w_2 = K_2 \sin^2(\varphi - \beta) - H_x M_2 \cos\varphi, \quad (2)$$

where K_2 is the uniaxial anisotropy constant of the second magnetic layer.

Volumetric density of two magnetic layers averaged over the layer thickness is

$$w = t_1 w_1 + t_2 w_2, \tag{3}$$

where

$$t_1 = \frac{h_1}{h_1 + h_2}, \qquad t_2 = \frac{h_2}{h_1 + h_2}. \tag{4}$$

Substituting (1) and (2) into (3), obtain

$$w = K \sin^2(\varphi - \beta) - \frac{3}{2}\sigma\lambda \sin^2\varphi - H_x M \cos\varphi, \tag{5}$$

where K is the thickness-averaged anisotropy constant,

$$K = t_1 K_1 + t_2 K_2, \tag{6}$$

M is the thickness-averaged magnetization vector,

$$M = t_1 M_1 + t_2 M_2, \tag{7}$$

λ is the thickness-averaged magnetostriction constant,

$$\lambda = \lambda_1 t_1. \tag{8}$$

Let us introduce the constants of the equivalent fields of anisotropy H_{an} and magnetostriction H_σ according to the following formulas:

$$H_{an} = 2\frac{t_1 K_1 + t_2 K_2}{M_{eff}}, \tag{9}$$

$$H_\sigma = 2t_1 \frac{3}{2M_{eff}} \sigma\lambda_1. \tag{10}$$

Then the volumetric magnetic energy density takes the following form:

$$w = M\left[\frac{H_{an}}{2}\sin^2(\varphi - \beta) - \frac{H_\sigma}{2}\sin^2\varphi - H_x\cos\varphi\right]. \tag{11}$$

Using the basic trigonometric relationships and equation $\beta = \pi/4$, obtain

$$\sin^2(\varphi - \beta) = \frac{1 - \cos 2(\varphi - \beta)}{2} = \frac{1 - \sin 2\varphi}{2}. \tag{12}$$

Substituting (12) into (11) and taking constant H_{an} out of the square brackets, obtain for the magnetic energy density

$$w = MH_{an}\left[\frac{1 - \sin 2\varphi}{4} - \frac{h_\sigma}{2}\sin^2\varphi - h_x\cos\varphi\right], \tag{13}$$

where dimensionless quantities

$$h_\sigma = \frac{H_\sigma}{H_{an}}, \tag{14}$$

$$h_x = \frac{H_x}{H_{an}}. \tag{15}$$

have been introduced.

Equilibrium value of orientation angle φ of magnetization vector (7) will be determined by the minimum of magnetic energy density (13), i.e. by the solution of equation

$$\frac{\partial w}{\partial \varphi} = MH_{an}\left[-\frac{\cos 2\varphi}{2} + h_x\sin\varphi - h_\sigma\sin\varphi\cos\varphi\right] = 0. \tag{16}$$

Taking into account that

$$\cos 2\varphi = 1 - 2\sin^2\varphi, \tag{17}$$

equation (16) may be represented as

$$-\frac{1}{2} + \sin^2\varphi + h_x\sin\varphi - h_\sigma\sin\varphi\cos\varphi = 0. \tag{18}$$

Transposing the last term in (18) to the right and squaring both sides of the resulting equality, transform this equation into a fourth-order polynomial equation for $\sin\varphi$:

$$x^4 + 2\frac{h_x}{1 + h_\sigma^2}x^3 + \frac{h_x^2 - 1 - h_\sigma^2}{1 + h_\sigma^2}x^2 - \frac{h_x}{1 + h_\sigma^2}x + \frac{1}{4(1 + h_\sigma^2)} = 0, \tag{19}$$

where the following designation is introduced:

$$x = \sin\varphi. \tag{20}$$

Generally, equation (19) may have four different real analytical solutions [4,9]. These solutions are expressed via elementary functions and have a cumbersome form; therefore, let us write them in the functional form:

$$x_1 = x_1(h_x, h_\sigma), \qquad x_2 = x_2(h_x, h_\sigma),$$

$$x_3 = x_3(h_x, h_\sigma), \qquad x_4 = x_4(h_x, h_\sigma). \tag{21}$$

Analysis of those solutions shows that in the parameter h_x range

$$-h_{cr} \leqslant h_x \leqslant h_{cr} \tag{22}$$

there exist four different real solutions (21). Here h_{cr} is some critical value of parameter h_x. For the h_x values beyond this range, only two real solutions are possible. Another interesting feature of solutions (21) of equation (19) is that for $h_\sigma > 0$ in range (22) two solutions, e.g. $x_1(h_x, h_\sigma)$ and $x_4(h_x, h_\sigma)$, correspond to two local minima of magnetic energy density (13), while the other two solutions $x_2(h_x, h_\sigma)$ and $x_3(h_x, h_\sigma)$ correspond to local maxima. This case is considered in details in [4]. When $h_\sigma < 0$, tensile deformation is observed, and the solution for magnetic energy density (13) minima and maxima gets inverted, $x_1(h_x, h_\sigma)$ and $x_4(h_x, h_\sigma)$ will correspond to two local maxima of the magnetic energy density (13), while the other two solutions $x_2(h_x, h_\sigma)$ and $x_3(h_x, h_\sigma)$ will correspond to local minima. Just this is what explains the difference in the magnetoresistance dependence for the cases of compressive deformation ($h_\sigma > 0$) and tensile deformation ($h_\sigma < 0$).

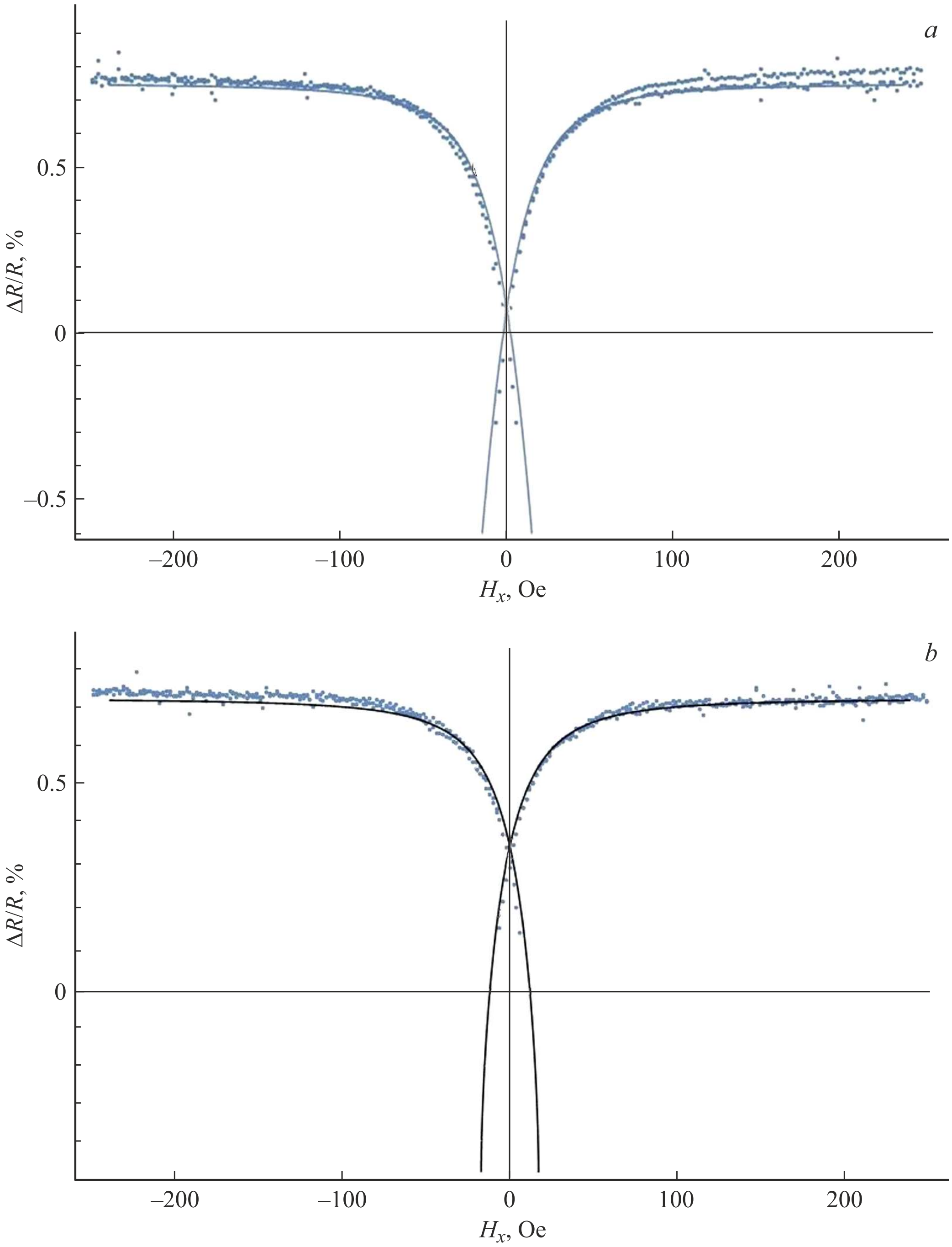

The experimental (dots) and theoretical (solid line) magnetic field dependences of relative magnetoresistance for different mechanical tensile stresses. *a* — without deformation, *b* — $\sigma = 30$ MPa, *c* — $\sigma = 65$ MPa, *d* — $\sigma = 100$ MPa.

Let us compare the theoretical and experimental data. According to the AMR effect, magnetoresistance of the FeNiCo magnetoresistive layer is defined as follows [10]:

$$R = R_{\perp}\left(1 + \frac{\Delta\rho}{\rho}\cos^2\phi\right), \tag{23}$$

where ϕ is the angle between current density vectors $\mathbf{J}$ and magnetization vector $\mathbf{M}_2$ in the strip, $R_{\perp}$ is the strip resistance in the direction perpendicular to vector $\mathbf{J}$, $\Delta\rho/\rho$ is the AMR effect coefficient. Since the experimentally measured relative variation in magnetoresistance is expressed in relative units and the curve itself may be shifted, let us approximate the relative magnetoresistance variation by formula

$$\frac{\Delta R}{R} = a\cos^2\varphi - b = a(1 - \sin^2\varphi) - b. \tag{24}$$

Substituting into (24) solution (21) corresponding to the minimum tensile-deformation magnetic energy ($h_\sigma < 0$),

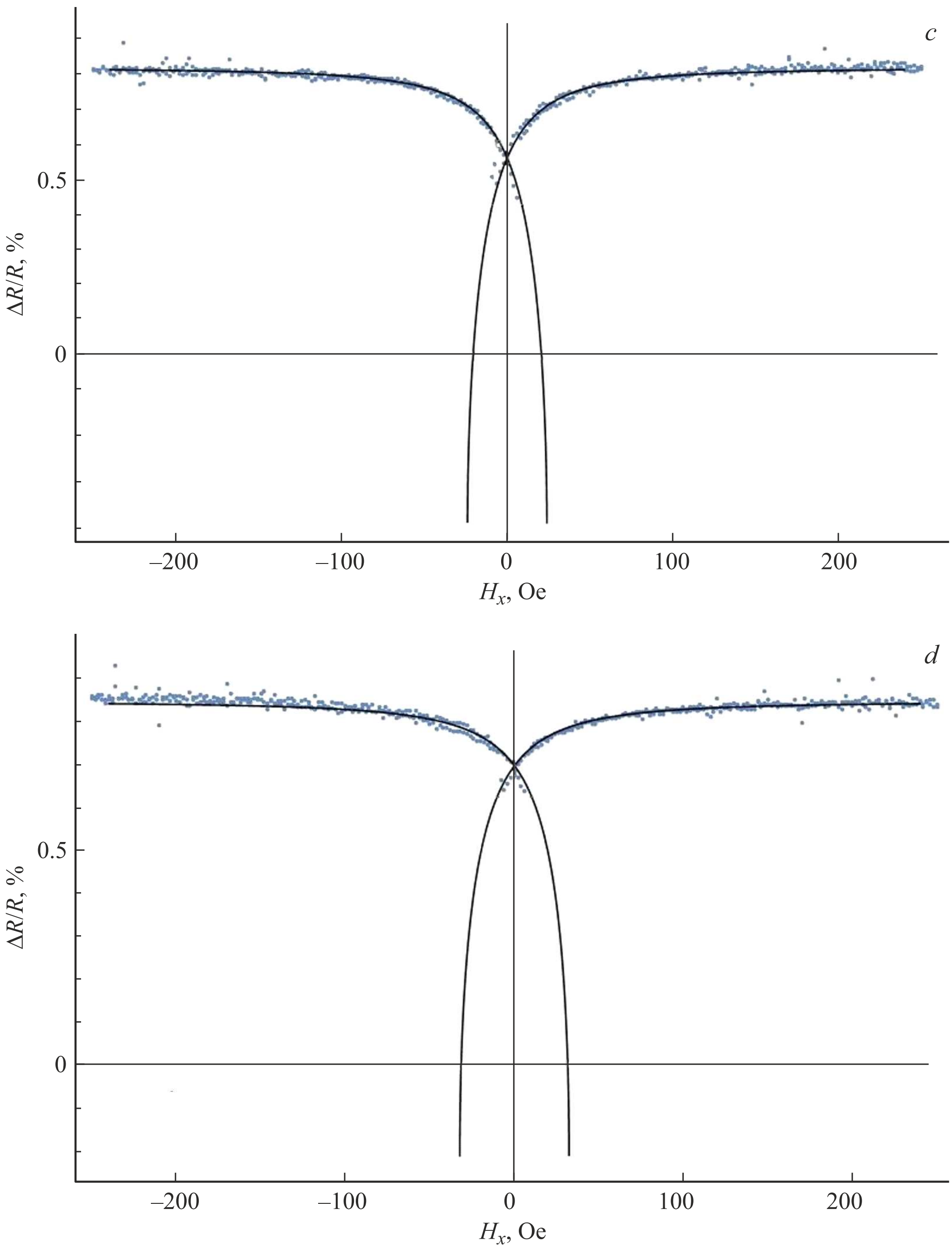

Figure (*continued*).

obtain

$$\frac{\Delta R}{R} = a\cos^2\varphi - b = a\left(1 - x_2\left(\frac{H_x}{H_{an}}, h_\sigma\right)\right) - b, \quad (25)$$

where designation (15) of h_x is used.

Next, approximating the experimental data given in [8] with function (25) using the least squares method and varying parameters a, b, h_σ, obtain the following parameter values corresponding to the best quadratic approximation at $H_{an} = 30\,\text{Oe}$.

In the absence of mechanical stress ($\sigma = 0\,\text{MPa}$):

$$a = 1.3535, \qquad b = 0.5943, \qquad h_\sigma = 0. \quad (26)$$

Under mechanical tensile stress $\sigma = 30\,\text{MPa}$:

$$a = 1.4060, \qquad b = 0.6325, \qquad h_\sigma = 0.4968. \quad (27)$$

Under mechanical tensile stress $\sigma = 65\,\text{MPa}$

$$a = 1.8380, \qquad b = 1.0203, \qquad h_\sigma = 1.0593. \quad (28)$$

Under mechanical tensile stress $\sigma = 100\,\text{MPa}$

$$a = 1.7782, \qquad b = 0.9306, \qquad h_\sigma = 1.5007. \quad (29)$$

The figure shows experimental and theoretical plots (as per (24), (25) and for parameters (26)−(29)) representing the relative magnetoresistance variations with external magnetic field H_x variations from −250 to 250 Oe and back. As shown by the theoretical dependencies for mechanical tensile stresses $\sigma = 0$, 30, 65, 100 MPa presented in the Figure panels $a-d$, the lowest magnetoresistance gets achieved at critical values of the external magnetic field $H_{cr} = H_{an}h_{cr} = 15$, 17.2, 24.5, 32.6 Oe, respectively. In the absence of the mechanical deformation, $H_{cr} = H_{an}/2$. When tensile strain is applied and further increased, H_{cr} also increases; at $\sigma = 100$ MPa, it slightly exceeds H_{an} and reaches 32.6 Oe.

Panels $a-d$ of the Figure demonstrate a good agreement between the experimental and theoretical curves. However, the theoretical curves drop sharply well below the experimental values. This may probably be explained by that in this region the local minimum of magnetic energy density (13) has an insignificant depth. Therefore, the so-oriented magnetic moment will be unstable and can reorient to another stable state with the lowest energy.

The proposed theoretical model provides a good quantitative agreement with experimental data and explains all the magnetoresistance behavior features under tensile deformation. This study has established that under the nanostructure magnetization reversal the experimental value of the maximum resistance variation caused by the AMR effect is lower than the theoretical one because of instability of the local state of the magnetic moment orientation in the vicinity of critical value $h_x = h_{cr}$. In the case of tensile deformation, the maximum magnetoresistance variation is achieved at the external magnetic field values close to critical value H_{cr}. The experimentally revealed asymmetry in the magnetoresistance variations under the tensile and compressive deformations has been explained. Note that the theory developed may be applied to similar structures based on the giant magnetoresistive effect provided it is appropriately adjusted taking into account physical characteristics of this effect.

Funding

The study was supported by the RF Ministry of Science and Higher Education (FNRM-2025-0005).

Conflict of interests

The authors declare that they have no conflict of interests.

References

[1] F. Miao, S.-J. Liang, B. Cheng, npj Quantum Mater., **6**, 59 (2021). DOI: 10.1038/s41535-021-00360-3

[2] I.V. Antonova, Phys. Usp., **65** (6), 567 (2022). DOI: 10.3367/UFNe.2021.05.038984.

[3] A.A. Bukharaev, A.K. Zvezdin, A.P. Pyatakov, Yu.K. Fetisov, Phys. Usp., **61** (12), 1175 (2018). DOI: 10.3367/UFNe.2018.01.03827.

[4] D.A. Zhukov, O.P. Polyakov, P.A. Polyakov, S.I. Kasatkin, V.V. Amelichev, D.V. Kostyuk, Phys. Met. Metallogr., **125** (10), 1072 (2024). DOI: 10.1134/S0031918X24601124.

[5] L.I. Naumova, A.A. Zakharov, M.A. Milyaev, N.G. Bebenin, R.S. Zavornitsyn, I.K. Maksimova, V.V. Proglyado, V.V. Ustinov, Phys. Met. Metallogr., **124** (3), 252 (2023). DOI: 10.1134/S0031918X22602141.

[6] G.S.C. Bermúdez, D. Makarov, Adv. Funct. Mater., **31** (39), 2007788 (2021). DOI: 10.1002/adfm.202007788

[7] B. Rivkin, C. Becker, F. Akbar, R. Ravishankar, D.D. Karnaushenko, R. Naumann, A. Mirhajivarzaneh, M. Medina-Sánchez, D. Karnaushenko, O.G. Schmidt, Adv. Intell. Syst., **3** (6), 2000238 (2021). DOI: 10.1002/aisy.202000238

[8] D. Zhukov, V. Amelichev, S. Kasatkin, D. Kostyuk, Sensors, **21** (17), 5785 (2021). DOI: 10.3390/s21175785

[9] G. Korn, T. Korn, *Spravochnik po matematike* (Nauka, M., 1973), s. 44–45. (in Russian)

[10] T.R. Mcguire, R.I. Potter, IEEE Trans. Magn., **11** (4), 1018 (1975). DOI: 10.1109/TMAG.1975.1058782

Translated by EgoTranslating